JOURNAL OF MATERIALS SCIENCE 22 (1987) 4362–4368

High-field superconductivity in Al–O–Pb and Al–O–Pb–Bi sputtered films

A. INOUE, K. MATSUZAKI, T. OGASHIWA*, T. MASUMOTO
The Research Institute for Iron, Steel and Other Metals, Tohoku University, Sendai 980, Japan

The sputter-quenched Al_xO_y alloys containing lead and bismuth elements, which are insoluble to aluminium, have been found to exhibit a remarkably enhanced upper critical field, H_{c2}, which is higher by about 6 to 66 times than those of pure lead metal and $Pb_{60}Bi_{40}$ alloy. The sputtered structure consists of amorphous Al_xO_y and f c c lead or h c p ε (lead–bismuth) phases. The lead and ε phases disperse homogeneously in the amorphous matrix and their particle sizes and interparticle distances are about 10 to 20 nm and 5 to 20 nm, respectively, for lead and ε particles. The superconducting transition temperature, T_c, upper critical magnetic field, H_{c2}, at 4.3 K, and residual resistivity at 10 K are 7.74 K, 3.3 T and 2.09×10^5 $\mu\Omega$ cm, respectively, for $(Al–O)_{92.8}Pb_{7.2}$ and 7.45 K, 8.2 T and 1.70×10^6 $\mu\Omega$ cm, respectively, for $(Al–O)_{86.2}(Pb_{0.6}Bi_{0.4})_{13.8}$. The remarkable enhancement of H_{c2} is interpreted as being mainly due to a remarkable decrease of the coherence length resulting from a large reduction of the effective mean free path of electrons. Additionally, the fluxoid pinning force under applied field has also been markedly enhanced for the duplex structure films than for sputtered lead film, probably because of the change of the dispersed lead phase into a type-II superconductor and an effective fluxoid pinning action at the interface between Al_xO_y and fine lead particles.

1. Introduction

During the last two years, we have performed a series of studies [1–8] on the preparation of duplex structure alloys with finely and homogeneously dispersed immiscible phase particles, by taking advantage of phase-separation phenomena in the equilibrium solid and/or liquid state, and their characterization. It has been found [3, 4, 6–8] that rapidly quenched Ge–Pb, Ge–Pb–Bi and Ge–Pb–Bi–Sn alloys consist of f c c lead, h c p ε (lead–bismuth) or ε + b c t tin + hexagonal bismuth particles embedded in a cubic germanium matrix and exhibit unique electrical properties, i.e. an upper critical magnetic field higher by about 10 to 100 times than that of pure lead metal [9] or ε-$Pb_{60}Bi_{40}$ [10] alloy and extremely high electrical resistivities of 7000 to 10000 $\mu\Omega$ cm at 250 K combined with positive and linear temperature variation as large as about 70 to 90% in the range from 10 to 273 K. These anomalous electrical properties have been thought to result from the duplex structure consisting of semiconductor and metal. This new information suggests the possibility that another type of duplex structure alloy, consisting of superconducting metallic phases embedded in an oxide or nitride matrix, also exhibits electrical properties with more enhanced anomaly, because the difference in the electrical properties between oxide or nitride and metal is more significant than that between semiconductor and metal. The aim of this paper is to examine the microstructure and superconducting properties of sputtered Al–O–Pb and Al–O–Pb–Bi films and to investigate the appropriateness of the general concept derived from the previous results [3, 4, 6–8] on rapidly quenched germanium-based alloys, i.e. the possibility of whether or not a superconductor with a remarkably enhanced H_{c2} and an extremely high electrical resistivity may be prepared for the oxide–metal mixed material.

2. Experimental procedure

$(Al–O)_xPb_{100-x}$ (x = 0, 36.1, 63.9, 87.5 and 92.8%) and $(Al–O)_x(Pb_{0.6}Bi_{0.4})_{100-x}$ (x = 0, 25.0, 58.7, 72.4, 79.3 and 86.2%) alloys were sputtered on a water-cooled ceramic substrate to form a rectangular film (3 mm × 10 mm) with a thickness of 20 to 30 μm using a radio frequency (r.f.) sputtering apparatus. The Al–O–Pb and Al–O–Pb–Bi films for transmission electron microscopic observation were sputtered on a rock salt substrate to form a thin foil of 100 nm thick. The target cathode consisted of highly pure Al_2O_3 and pure lead (99.99 wt %) metal or $Pb_{60}Bi_{40}$ alloy and the composition was controlled by changing the surface area ratio of the two raw materials. After evacuating the sputtering chamber mounted with the target material up to 2×10^{-5} Pa, argon gas of 4 Pa was fed through an automatic gas-flow controller to make argon plasma in the chamber. The argon plasma was generated between substrate cathode and stainless steel anode. The anode current usually supplied was 60 mA and the anode voltage was 1 kV. Prior to sputtering the target the substrate was

* *Present address*: Research and Development, Tanaka Denshi Kogyo Ltd, Mitaka 181, Japan.

0022–2461/87 $03.00 + .12

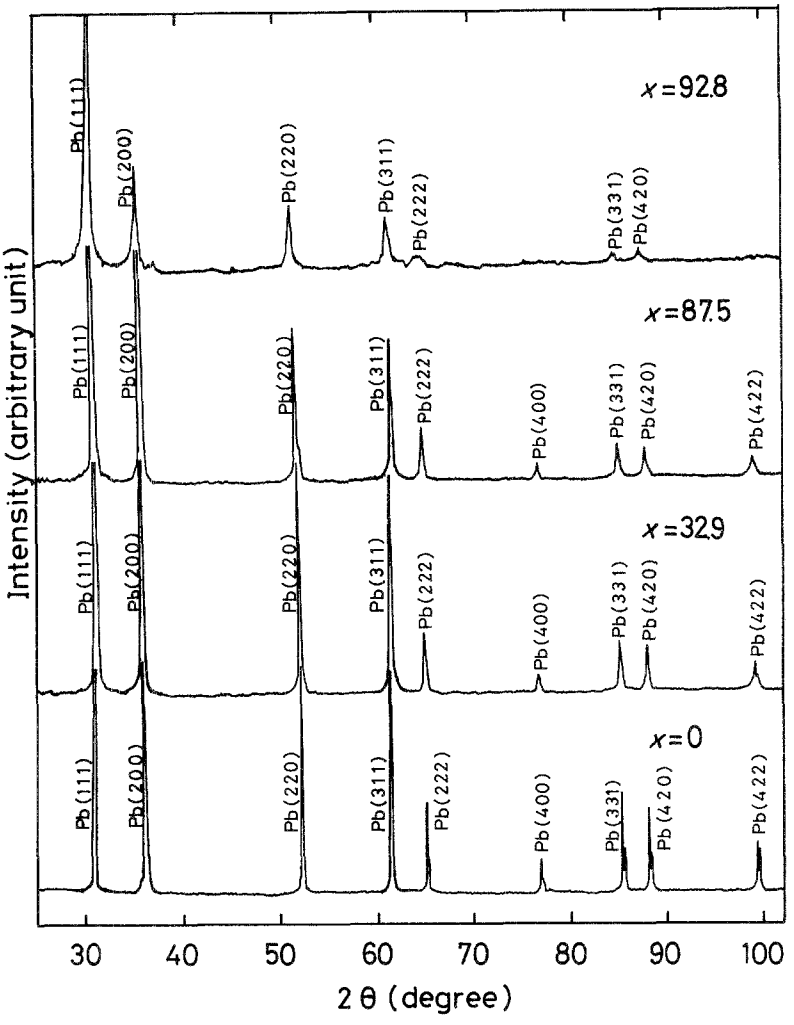

Figure 1 X-ray diffraction patterns of $(Al–O)_x Pb_{100-x}$ (x = 0, 32.9, 87.5 and 92.8%) sputtered films.

sputtered to clean its surface for 5 min by applying a negative bias against the substrate. The gap between the target and substrate was fixed at 20 mm.

The structure of the sputtered films was examined by X-ray diffractometry and transmission electron microscopy (TEM). Measurements of superconducting properties, i.e. transition temperature, T_c, upper critical magnetic field, H_{c2}(T), and critical current density, J_c(H), were made by the d.c. method using the four electrical probes. The magnetic field up to 8 T was applied transversely to the specimen surface and excited current. The temperature was measured using a calibrated germanium thermometer with accuracy better than ± 0.01 K. The capacitance thermometer (glass ceramic $SrTiO_3$) was also used in controlling and/or measuring the temperature under the fields.

3. Results

3.1. Sputtered structure

Figs 1 and 2 show the X-ray diffraction patterns of sputtered $(Al–O)_x Pb_{100-x}$ (x = 0, 32.9, 87.5 and 92.8%) and $(Al–O)_x(Pb_{0.6}Bi_{0.4})_{100-x}$ (x = 0, 25.0, 58.7, 79.3 and 86.2%) films. All the patterns can be identified as only fcc lead for Al–O–Pb alloys and hcp ε (lead–bismuth) + tetragonal X + hexagonal bismuth for Al–O–Pb–Bi alloys and no diffraction peaks corresponding to Al–O are seen. It is thus notable that lead and ε phases are formed even for the Al–O-rich films with x = 86 to 93%. Although the intensity of lead and ε diffraction peaks tends to decrease with decreasing lead and bismuth contents, there is no systematic variation in the peak position of lead and ε phases with area ratios of lead and lead + bismuth to Al_2O_3.

In order to examine the reason why no diffraction peaks of Al_xO_y in $(Al–O)_x Pb_{100-x}$ and $(Al–O)_x(Pb_{0.6}Bi_{0.4})_{100-x}$ films is detected, TEM observation was carried out for a deposited Al_xO_y thin film without lead and bismuth. Fig. 3 shows a bright-field electron micrograph and a selected-area diffraction pattern of a sputtered Al_xO_y film. No distinct contrast revealing the existence of crystalline phase is seen in the bright-field image and the diffraction pattern consists only of broad halo rings, indicating that the sputtered Al_xO_y film is composed of an amorphous phase. From this result, it appears reasonable to consider that the structure of $(Al–O)_x Pb_{100-x}$ and $(Al–O)_x(Pb_{0.6}Bi_{0.4})_{100-x}$ films prepared under the same sputtering conditions consists of amorphous Al_xO_y oxide and lead or ε + X + bismuth phases. The lattice parameters of lead and ε phases in $(Al–O)_x Pb_{100-x}$ and $(Al–O)_x(Pb_{0.6}Bi_{0.4})_{100-x}$ films are presented as a function of area ratios of lead or $Pb_{60}Bi_{40}$ to Al_2O_3 in the target in Fig. 4. The lattice parameters remain constant, i.e. 0.4951 nm for lead and a = 0.3500 nm and c = 0.5552 nm for ε (lead–bismuth), over the whole composition range, and agree with those of pure lead [11] metal and ε-$Pb_{60}Bi_{40}$ [11] alloy. It is therefore concluded that no dissolution of aluminium and/or oxygen into lead and ε phases is detected even for the Al_xO_y-rich films, in accordance with expectation from Al–Pb and Al–Bi equilibrium phase diagrams [12].

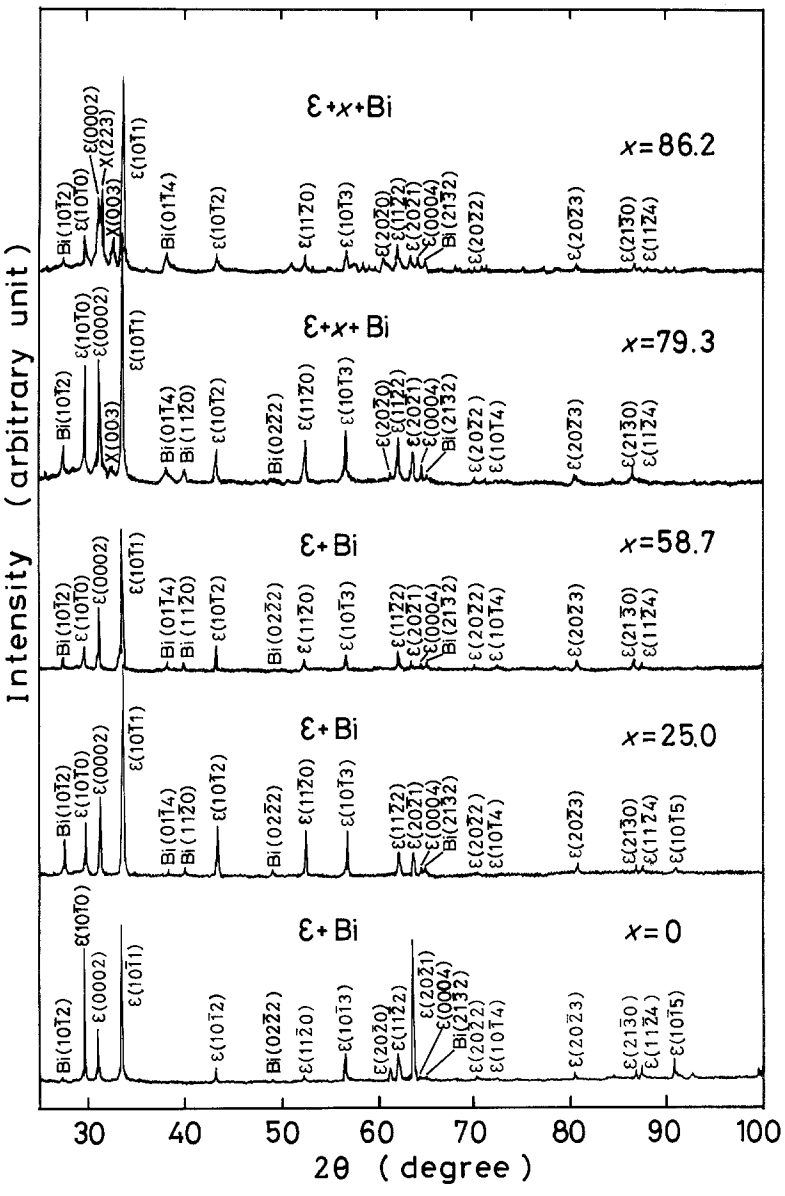

Figure 2 X-ray diffraction patterns of $(Al–O)_x(Pb_{0.6}Bi_{0.4})_{100-x}$ (x = 0, 25.0, 58.7, 79.3 and 86.2%) sputtered films.

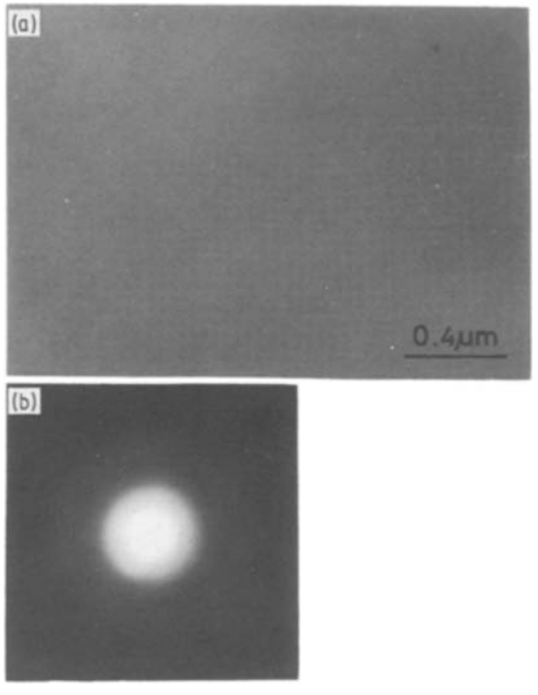

Figure 3 (a) Bright-field electron micrograph and (b) selected-area diffraction pattern of an Al_xO_y sputtered film.

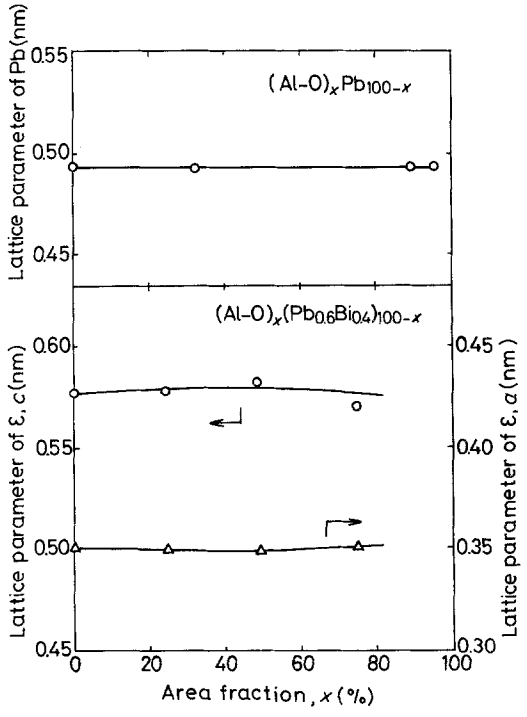

Figure 4 Change in the lattice parameter of fcc lead and hcp ε (lead–bismuth) in $(Al–O)_xPb_{100-x}$ and $(Al–O)_x(Pb_{0.6}Bi_{0.4})_{100-x}$ sputtered films with area ratio of Al_2O_3 in the sputtered target.

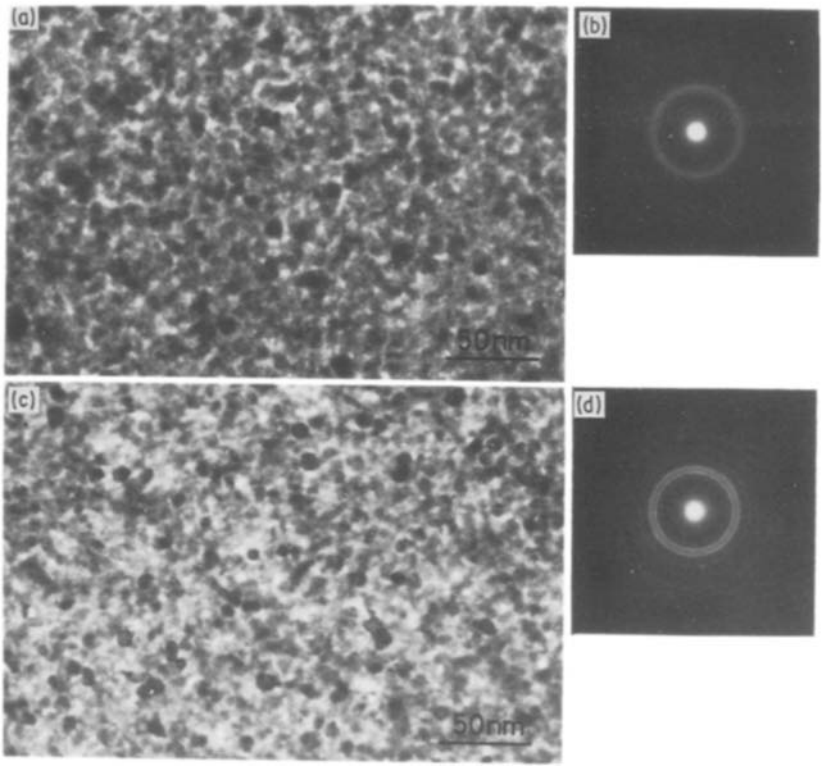

Figure 5 Bright-field electron micrographs and selected-area diffraction patterns of (a, b) $(Al–O)_{85.6}Pb_{14.4}$ and (c, d) $(Al–O)_{79.3}(Pb_{0.6}Bi_{0.4})_{20.7}$ sputtered films.

Fig. 5 shows the bright-field electron micrographs and selected-area diffraction patterns of sputtered $(Al–O)_{87.5}Pb_{12.5}$ and $(Al–O)_{79.3}(Pb_{0.6}Bi_{0.4})_{20.7}$ films. The diffraction patterns revealed the coexistence of amorphous Al_xO_y and f c c lead phases for the former film and of amorphous Al_xO_y and h c p ε for the latter film, being consistent with the results derived from X-ray diffractometry. The average particle size and interparticle spacing of the lead phase are about 10 to 20 nm and 10 to 20 nm, respectively, for $(Al–O)_{87.5}Pb_{12.5}$ and about 10 to 15 nm and 5 to 15 nm, respectively, for $(Al–O)_{79.3}(Pb–Bi)_{20.7}$. From the above results, it is concluded that the $(Al–O)_xPb_{100-x}$ and $(Al–O)_x(Pb_{0.6}Bi_{0.4})_{100-x}$ films have the duplex structure consisting of f c c lead or h c p ε (lead–bismuth) particles embedded finely and homogeneously in Al_xO_y amorphous oxide.

3.2. Superconducting properties

Fig. 6 shows typical normalized electrical resistance (R/R_n) curves in the vicinity of T_c as a function of temperature for sputtered $(Al–O)_xPb_{100-x}$ films. Here R_n is the residual resistance at 10 K in the normal state.

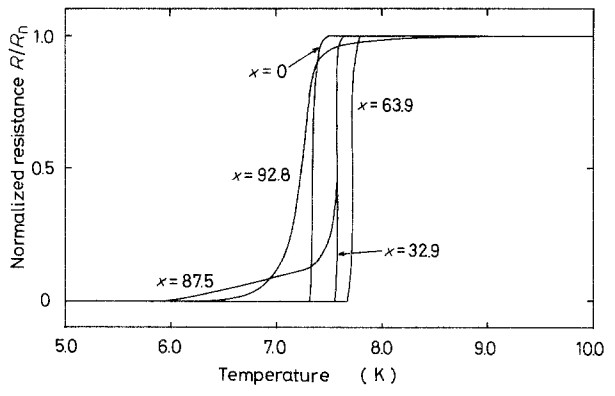

Figure 6 Normalized electrical resistance R/R_n as a function of temperature for $(Al–O)_xPb_{100-x}$ sputtered films.

It is seen that all the films translate rather sharply into a superconducting state. It is noted that the superconducting transition for the Al–O–Pb alloys with composition x = 32.9, 63.9 and 87.5% occurs at temperatures higher than T_c of lead metal itself. The changes in T_c and ΔT_c with area fraction of Al_2O_3, x, are shown in Fig. 7 for $(Al–O)_xPb_{100-x}$ and in Fig. 8 for $(Al–O)_x(Pb_{0.6}Bi_{0.4})_{100-x}$. Here T_c was taken as the temperature at $R/R_n = 0.5$ and ΔT_c as the temperature interval between $0.1R_n$ and $0.9R_n$. T_c of the Al–O–Pb films is 7.36 K at x = 0%, shows a maximum value of 7.74 K at x = 63.9% and then decreases to 7.24 K at 92.8%. On the other hand, T_c of the Al–O–Pb–Bi films is 9.07 K at x = 0%, decreases gradually with increasing x content, e.g. to 7.45 K at x = 57.8%, and remains unchanged at compositions above 60%x. No enhancement of T_c is seen for the duplex alloys containing lead–bismuth particles, in good contrast to the result for the Al–O–Pb duplex alloys. ΔT_c of Al–O–Pb films remains constant (about 0.05 K) in the composition range below 65%x and increases with further increasing x content to 0.4 K at x = 92.8% whereas that of the Al–O–Pb–Bi films increases from 0.03 K at x = 0% to 1.4 K at compositions above 60%. Fig. 9 shows the change in the residual electrical resistivity at 10 K as a function of area fraction, x, for sputtered Al–O–Pb films. The resistivity increases gradually in the range below about 50%x and rapidly in the range above 60%x and reaches as high as about 1.26×10^7 $\mu\Omega$cm at 92.7%x. It is noticed that $(Al–O)_{92.8}Pb_{7.2}$ film is a superconductor combined with an extremely high electrical resistivity ($\simeq 10^7$ $\mu\Omega$cm). The details of the electrical resistive behaviour of sputtered Al–O–Pb films as a function of temperature and applied magnetic field have been presented elsewhere [7].

Fig. 10 plots the upper critical magnetic field, H_{c2}, of sputtered $(Al–O)_xPb_{100-x}$ films as a function of

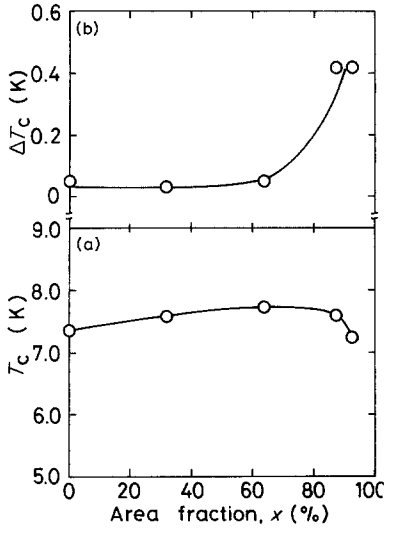

Figure 7 Changes in (a) superconducting transition temperature T_c and (b) transition width ΔT_c with area ratio of Al_2O_3 in the target for $(Al–O)_xPb_{100-x}$ sputtered films.

temperature. H_{c2} increases largely with decreasing temperature and increasing x content. The temperature dependence of H_{c2} is almost linear for pure lead metal, but the temperature gradient for the Al–O–Pb films changes from a larger slope in the range of $0.8 \leqslant t = T/T_c \leqslant 1.0$ to a smaller slope in the range of $0.5 \leqslant t = T/T_c \leqslant 0.8$. It is noticed that the H_{c2} of $(Al–O)_{92.8}Pb_{7.2}$ film is 66 times larger than that ($\simeq 0.05T$ at 4.2 K) [9] of pure lead film. A similar remarkable enhancement of H_{c2} is also observed for sputtered $(Al–O)_x(Pb_{0.6}Bi_{0.4})_{100-x}$ films as shown in Fig. 11. The temperature gradient of H_{c2}(T) increases with increasing x concentration and H_{c2} at 4.2 K for $(Al–O)_{86.2}(Pb_{0.6}Bi_{0.4})_{13.8}$ film is as high as ~ 8.2 T, being 5.5 times higher than that (1.5 T at 4.2 K) [10] of sputtered $Pb_{60}Bi_{40}$ film. Thus there is a clear tendency in the sputtered Al–O–Pb and Al–O–Pb–Bi films that

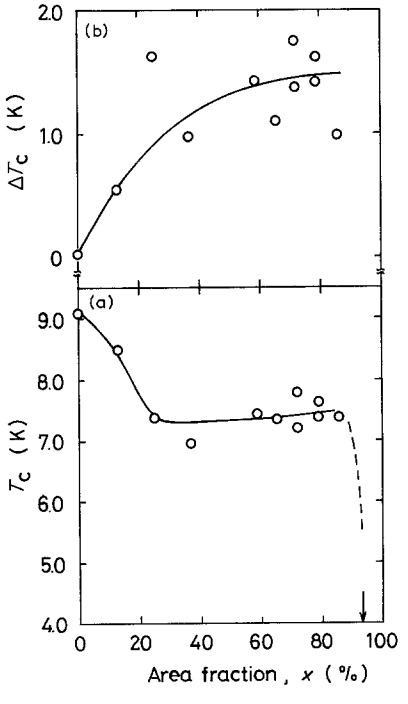

Figure 8 Changes in (a) superconducting transition temperature T_c and (b) transition width ΔT_c with area ratio of Al_2O_3 in the target for $(Al–O)_x(Pb_{0.6}Bi_{0.4})_{100-x}$ sputtered films.

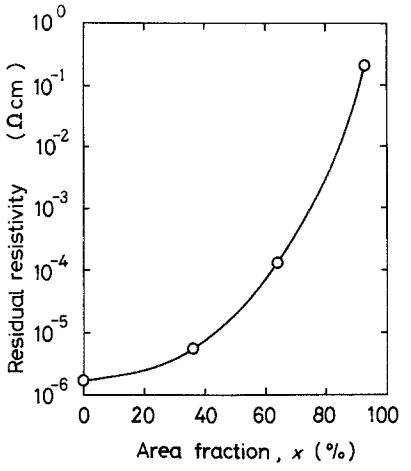

Figure 9 Change in residual electrical resistivity at 10 K with area ratio of Al_2O_3 in the target for $(Al–O)_xPb_{100-x}$ sputtered films.

the higher the residual electrical resistivity the higher is H_{c2}.

Fig. 12 shows the critical current density at 4.27 K as a function of transversely applied magnetic field for sputtered $(Al–O)_{85.6}Pb_{14.4}$ film. The J_c value is 4.1×10^5 A m^{-2} at $H = 0$ and 2.2×10^3 A m^{-2} at $H = 3$ T for the Al–O–Pb film and 5.8×10^7 A m^{-2} at $H = 0$ and 0 A m^{-2} at $H = 0.3$ T for sputtered pure lead film, indicating a marked difference of J_c values under an applied field above about 0.13 T between the Al–O–Pb and the lead films. This result suggests that the lead phase embedded in Al_xO_y amorphous phase changed from a type-I superconductor to a type-II superconductor. Considering the result that the real volume fraction occupied by superconducting lead phase is much smaller for the Al–O–Pb film, it is concluded that the fluxoid pinning force under an applied field is remarkably enhanced by the formation of coexisting amorphous Al_xO_y and fcc lead phases. The remarkable enhancement is presumably because lead phase embedded in an amorphous Al_xO_y matrix changes into a type-II superconductor and the interface between lead and Al_xO_y phases acts as an effective fluxoid pinning site.

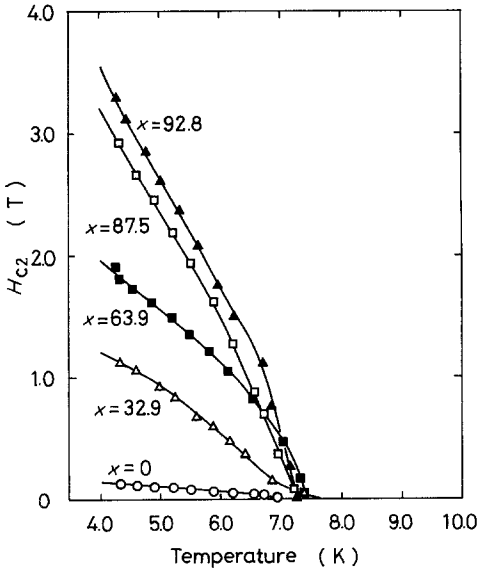

Figure 10 Upper critical magnetic field H_{c2} as a function of temperature for $(Al–O)_xPb_{100-x}$ sputtered films. I_s = 1 to 10 mA.

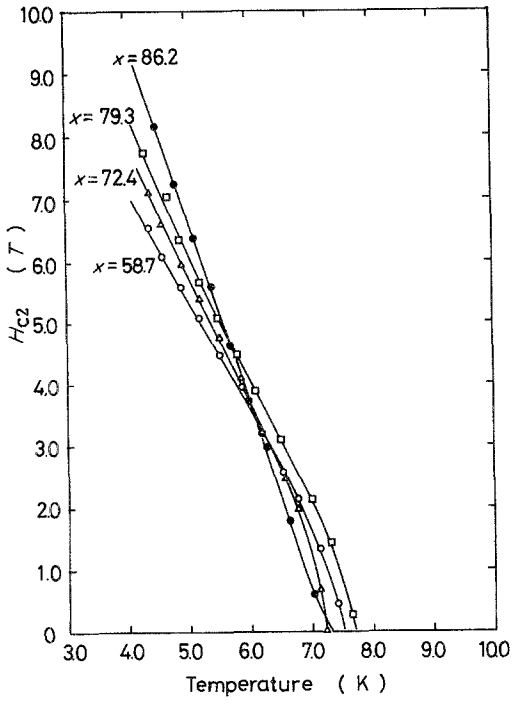

Figure 11 Upper critical magnetic field H_{c2} as a function of temperature for $(Al–O)_x(Pb_{0.6}Bi_{0.4})_{100-x}$ sputtered films. I_s = 1 to 10 μA.

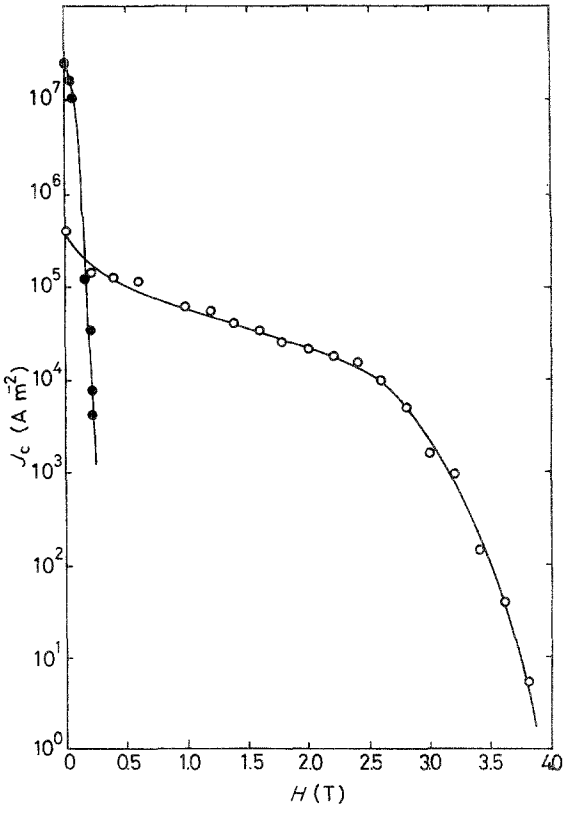

Figure 12 Critical current density J_c at 4.27 K as a function of applied field for (○) $(Al–O)_{85.6}Pb_{14.4}$ and (●) lead sputtered films.

4. Discussion

From the X-ray diffraction and transmission electron micrographic data shown in Figs 1 to 5, it is concluded that the sputtered Al–O–Pb and Al–O–Pb–Bi films consist of the duplex structure including fine lead or ε (lead–bismuth) particles in Al_xO_y matrix. Cohen and Douglass [13] have investigated the possibility of superconductivity for the sandwich material consisting of metal–insulator–metal phases and predicted that the superconductivity appears in principle for all the superconducting metals by an electron tunnelling effect from the metal into the insulator. Furthermore, the prediction has been confirmed for a number of thin film materials consisting of metal and oxide prepared by admitting controlled amounts of oxygen into the evaporation system during the evaporation of the metals [14]. Accordingly, the superconductivity for the present Al–O–Pb and Al–O–Pb–Bi alloys is considered as due to a mechanism similar to that [13] proposed for two superimposed metal films separated by an insulating oxide barrier. That is, the conduction electrons in lead and ε phases can tunnel so that a superconducting circuit is formed in the Al_xO_y–lead or ε duplex materials.

Next we discuss the reason for the significant enhancement of $H_{c2}(T)$ for sputtered Al–O–Pb and Al–O–Pb–Bi alloys. The residual electrical resistivities are as high as 10^7 $\mu\Omega$cm for the Al_xO_y-rich alloys, indicating that these alloys belong to an extremely "dirty" type-II superconductor. The linearized Ginzburg–Landau equation has been known [15] to lead to the following basic relation for $H_{c2}(T)$,

$$H_{c2} = \kappa 2^{1/2} H_c(T) = \phi_0/2\pi\xi^2(T) \quad (1)$$

where κ is the Ginzburg–Landau parameter, $H_c(T)$ the thermodynamic critical field, ϕ_0 the flux quantum and $\xi(T)$ the temperature dependent coherence length. The $\xi(T)$ is expressed by Equation 2 in the "dirty" limit $l_{eff} \ll \xi_0$ [16]

$$\xi(T) = 0.85[\xi_0 l_{eff} T_c/(T_c - T)]^{1/2} \quad (2)$$

where l_{eff} is an effective mean free path and ξ_0 is the BCS coherence length. Equations 1 and 2 indicate that H_{c2} for the superconductor consisting of lead or ε phase embedded in an Al_xO_y matrix increases with increasing $1/l_{eff}$ which is proportional to residual electrical resistivity.

A similar expression for H_{c2} has been proposed [17] for the duplex material in which superconducting metallic phases exist as spatially separated grains, in a highly electrical resistant matrix, connected by electron tunnelling

$$H_{c2}(T) = (3/2\pi^2)\phi_0/\xi_0 l_{eff} \quad (3)$$

In the free-electron model, the coherence length of an alloy ξ_0 can be estimated by

$$\xi_0 = \xi_{0p}(n/n_p)^{1/3} T_{cp}/T_c \quad (4)$$

where ξ_{0p} is the coherence length of the pure material, and n_p and n are the electron concentrations of the pure lead or ε (lead–bismuth) and the duplex structure alloy, respectively. T_{cp} and T_c are the transition temperatures of the pure lead or ε and the duplex structure alloy, respectively. Using the data of King *et al.* [18], ξ_0/ξ_{0p} is evaluated to be about 0.8.

It is very difficult to evaluate the l_{eff} value of superconducting lead and ε phases isolately embedded in an amorphous Al_xO_y matrix from residual electrical resistivities of the duplex Al–O–Pb and Al–O– Pb–Bi alloys. However, it is possible to evaluate l_{eff} using the measured values of $H_{c2}(T)$ and T_c under the assumption that Equations 1 to 4 are

valid for the present duplex superconductor. The l_{eff} values evaluated from Equations 1 and 3 are, respectively, 0.72 and 0.014 nm for $(Al–O)_{92.8}Pb_{7.2}$, 0.79 and 0.016 nm for $(Al–O)_{87.5}Pb_{12.5}$, 0.78 and 0.022 nm for $(Al–O)_{86.2}(Pb_{0.6}Bi_{0.4})_{13.8}$, and 0.11 and 0.022 nm for $(Al–O)_{79.3}(Pb_{0.6}Bi_{0.4})_{20.7}$. These values are comparable to minimum values of the mean free path of electrons of the superconducting lead and lead–bismuth phases. The anomalously high upper critical field for the sputtered Al_xO_y-based alloys is presumably due to an extremely short distance of the effective mean free path of electrons. Furthermore, the short mean free path is thought to result from a unique structural modification caused by sputter quenching, i.e. the superconducting lead and ε (lead-bismuth) particles disperse finely (within an interparticle distance of 10 to 20 nm) and isolately in a highly electrical resistant Al_xO_y matrix and contain a high density of quenching-induced internal defects. Additionally, the high stability in superconducting circuits caused by easy achievement of the tunnel effect resulting from homogeneous and fine dispersion of the immiscible second-phase particles, appears to be another reason for the remarkably enhanced H_{c2}. Finally, it appears important to point out that the small l_{eff} values derived from Equations 1 and 3 are of the same order as atomic radii and H_{c2} has been ideally enhanced for the present Al_xO_y alloys with the unique duplex structure prepared by sputter quenching.

From the above results and discussions, it might be concluded that the anomalously enhanced upper critical field originates from the modification of the microstructure in the Al–O–Pb and Al–O–Pb–Bi alloys by sputter quenching. These systems may provide a model system by which study of the percolating superconductivity and/or the interference effect between the electron localization and dirty-limit superconductivity may be made. The subsequent investigation is in progress in an attempt to determine unambiguously the predominant mechanism for the high-field superconductivity by sputter quenching.

5. Conclusion

Al_xO_y-based duplex films exhibiting a markedly enhanced superconductivity were prepared in $(Al–O)_x Pb_{100-x}$ (x = 0, 36.1, 63.9, 87.5 and 92.8%) and $(Al–O)_x(Pb_{0.6}Bi_{0.4})_{100-x}$ (x = 0, 20.0, 58.7, 72.4, 79.3 and 86.2%) systems by the sputtering technique. The duplex films consisted of amorphous Al_xO_y matrices and particulate fcc lead or hcp ε (lead–bismuth) phases. The particle sizes and the interparticle distances are about 10 to 20 nm and about 5 to 20 nm, respectively, for the Al–O–Pb and Al–O–Pb–Bi films.

These duplex films were found to exhibit superconductivity, presumably because of the tunnelling effect resulting from the finely dispersed lead or ε (lead–bismuth) particles. The transition temperature, T_c, was independent of composition and was in the range 7.24 to 7.74 K for the Al–O–Pb films and 7.45 to 9.07 K for the Al–O–Pb–Bi films. The upper critical field at 4.3 K increases continuously with increasing Al–O content in the range 1.1 to 3.3 T for the Al–O–Pb films and 6.0 to 8.2 T for the Al–O–Pb–Bi films. It is particularly noticeable that their H_{c2} values are 6 to 66 times higher than those of pure lead metal and $Pb_{60}Bi_{40}$ alloy. The remarkable enhancement of H_{c2} is interpreted being due mainly to a remarkable reduction of the coherence length resulting from a marked decrease of the effective mean free path of electrons. The critical current density J_c for $(Al–O)_{85.6}Pb_{14.4}$ film was of the order of 2.2×10^3 A m^{-2} at H = 3 T and 4.3 K, being much higher than those of pure lead metal and sputtered lead film. It is thus very important from scientific and engineering points of view that the duplex structure films consisting of fine lead or ε particles dispersed uniformly in the Al_xO_y amorphous matrix can be produced by sputtering Al_2O_3 containing lead and bismuth which are immiscible in aluminium in the equilibrium state, and that these duplex films exhibit superconducting properties with markedly enhanced H_{c2} which cannot be obtained for the dispersed superconducting metal and alloy themselves.

References

1. A. INOUE, M. OGUCHI, K. MATSUZAKI and T. MASUMOTO, *Int. J. Rapid Solid.* **1** (1984-85) 273.
2. A. INOUE, M. OGUCHI, K. MATSUZAKI, Y. HARAKAWA and T. MASUMOTO, *J. Mater. Sci.* **21** (1986) 260.
3. A. INOUE, M. OGUCHI, K. MATSUZAKI and T. MASUMOTO, *Int. J. Rapid Solid.* **2** (1986) 175.
4. K. MATSUZAKI, A. INOUE, M. OGUCHI, N. TOYOTA and T. MASUMOTO, *ibid.* **2** (1987) 231.
5. A. INOUE, N. YANO, K. MATSUZAKI and T. MASUMOTO, *J. Mater. Sci.* **22** (1987) 1827.
6. A. INOUE, M. OGUCHI, K. MATSUZAKI, T. OGASHIWA and T. MASUMOTO, *Sci. Rep. Res. Inst. Tohoku Univ.* **33** (1986) 111.
7. A. INOUE, T. OGASHIWA, K. MATSUZAKI and T. MASUMOTO, *J. Mater. Sci.* **22** (1987) 2063.
8. A. INOUE, K. MATSUZAKI and T. MASUMOTO, Proceedings of Korea-Japan Metals Symposium on Rapid Solidification Processing, edited by Korea Institute of Metals, Seoul, 1986, p. 45.
9. J. D. LIVINGSTON, *Phys. Rev.* **129** (1963) 1943.
10. J. E. EVETTS and J. M. A. WADE, *J. Phys. Chem. Solids* **31** (1970) 973.
11. W. B. PEARSON, "Handbook of Lattice Spacings and Structures of Metals and Alloys" (Pergamon, London, 1958) pp. 127, 156.
12. M. HANSEN, "Constitution of Binary Alloys" (McGraw-Hill, New York, 1958) pp. 74, 122.
13. M. H. COHEN and D. H. DOUGLASS Jr, *Phys. Rev. Lett.* **19** (1967) 118.
14. M. STRONGIN and O. F. KAMMERRER, *J. Appl. Phys.* **39** (1968) 2509.
15. R. KOEPKE and G. BERGMANN, *Z. Physik* **242** (1971) 33.
16. P. G. de GENNES, "Superconductivity in Metals and Alloys" (Benjamin, New York, 1966) p. 217.
17. N. K. HINDLEY and J. H. P. WATSON, *Phys. Rev.* **183** (1969) 52.
18. H. W. KING, C. M. RUSSELL and J. A. HULBERT, *Phys. Lett.* **20** (1966) 600.

Received 29 January
and accepted 15 April 1987